

Original Articles

Microbial hierarchical correlations and their contributions to carbon-nitrogen cycling following a reservoir cyanobacterial bloom

Yuanyuan Xue^a, Min Liu^a, Huihuang Chen^a, Erik Jeppesen^{b,c,d,e}, Hongteng Zhang^a,
Kexin Ren^a, Jun Yang^{a,*}

^a Aquatic EcoHealth Group, Fujian Key Laboratory of Watershed Ecology, Key Laboratory of Urban Environment and Health, Institute of Urban Environment, Chinese Academy of Sciences, Xiamen 361021, China

^b Department of Ecoscience, Aarhus University, Vejlsovej 25, 8600 Silkeborg, Denmark

^c Sino-Danish Centre for Education and Research, Beijing 100049, China

^d Limnology Laboratory, Department of Biological Sciences and Centre for Ecosystem Research and Implementation, Middle East Technical University, Ankara, Turkey

^e Institute of Marine Sciences, Middle East Technical University, Mersin, Turkey



ARTICLE INFO

Keywords:

Cross-trophic correlations
Protist
Bacterial lifestyle
Keystone taxa
Plankton community

ABSTRACT

Unraveling how microbial co-occurrences respond to cyanobacterial blooms is central to our understanding of the stability of aquatic ecosystems. Here, we examined the effects of a *Microcystis* bloom on the inter-domain eukaryotic and two size-fractionated bacterial networks in a subtropical reservoir. Eukaryotes, especially protists, had a central role in microbial networks, followed by particle-attached (PA) bacteria and free-living (FL) bacteria. Eukaryotes had more negative correlations with PA bacteria than with FL bacteria. The environmental changes related to the *Microcystis* bloom (i.e., water temperature, pH, chlorophyll *a*, total carbon, total organic carbon and nitrite nitrogen) strongly affected eukaryotes and PA bacteria network as reflected by the dynamics of community composition in major modules. Importantly, the network complexity and stability significantly increased in the post-bloom periods, and eukaryotes (especially protists) enhanced the stability of the microbial network. Compared to keystone FL bacteria, eukaryotic and PA bacterial hubs mainly determined the network structure and key functional potentials (i.e., nitrogen cycling, carbon fixation and carbon degradation). Thus, some keystone eukaryotes and PA bacteria might be used as indicators of the structure and function stability of microbial communities in reservoir ecosystems. Our study highlights the importance of considering microbial cross-kingdom and multiple size-fractionation correlations in evaluating the effects of environmental disturbances on microbial networks.

1. Introduction

Aquatic microbes, including eukaryotes and bacteria, are of paramount importance for community assembly and ecosystem function (Worden et al., 2015; Xue et al., 2018). They form complex ecological interactions (e.g., predation, mutualism, and parasitism) through materials, energy and information exchanges (Baltar et al., 2016; Bjorbækmo et al., 2020; Grujcic et al., 2018). Identifying and defining their interactions is critical for the understanding of how these complex microbial communities respond to and recover from disturbances, such as algal blooms (Woodhouse et al., 2016). Global expansion of harmful cyanobacterial blooms in inland waters, which arises from human activities and global warming, is one of the most profound disturbances to

aquatic microorganisms at present (Huisman et al., 2018; Paerl and Barnard, 2020).

Cyanobacterial blooms can influence the properties (e.g., colonization and degradation) of aquatic particles (Xu et al., 2016). Microorganisms enriched on particles have different composition and life history strategies (e.g., extracellular enzyme activity, production and respiration) from free-living microorganisms (Mestre et al., 2017). Some ecologists use 3- μ m pore-size filters to distinguish particle-attached bacteria (PA) from free-living bacteria (FL) in waters (Eloe et al., 2011; Ganesh et al., 2014; Liu et al., 2019b). We have investigated the eukaryotic and different lifestyles bacterial communities during a reservoir cyanobacterial bloom. Interestingly, these microbial communities showed clear patterns from bloom to post-bloom periods (Liu

* Corresponding author.

E-mail address: jyang@iue.ac.cn (J. Yang).

<https://doi.org/10.1016/j.ecolind.2022.109401>

Received 17 April 2022; Received in revised form 17 August 2022; Accepted 30 August 2022

Available online 8 September 2022

1470-160X/© 2022 The Author(s). Published by Elsevier Ltd. This is an open access article under the CC BY-NC-ND license (<http://creativecommons.org/licenses/by-nc-nd/4.0/>).

et al., 2019b; Xue et al., 2018). Although numerous studies have elucidated how algal blooms affect microbial co-occurrence between eukaryotic plankton and bacteria in bulk water samples (Baltar et al., 2016; Mikhailov et al., 2019), we still lack a comprehensive understanding of whether and how such blooms impact the inter-domain ecological network of eukaryotes (protists, fungi and metazoa) and bacteria associated to discrete size-fractions (FL and PA).

Our understanding of microbial interactions in natural environments is limited in part because most of these microbes are unculturable (Zhou et al., 2010). Network analyses, however, are now widely applied to explore microbial connections within the domain or among different domains or different trophic levels in natural ecosystems (Chafee et al., 2018; Liu et al., 2019a; Zhou et al., 2021). Among these, molecular ecological network analyses (MENA) can relate network topological features with environmental factors, and show robustness against data noise (Deng et al., 2012). For example, Yuan et al. (2021) have shown that climate warming significantly increased microbial network complexity and stability, further strengthening microbial community function using MENA. Network modular structures are clusters of highly inter-connected microbes and these co-varying biota may have similar environmental preferences or niches (Chafee et al., 2018; Zhou et al., 2021). Additionally, network analysis can discern the role of every node, which was classified as network hubs, module hubs, connectors and peripherals (Guimerà and Amaral, 2005). These keystone species can act as indicators of community stability in natural lakes (Liu et al., 2022). Despite this knowledge and an increasing use of network analysis in microbial ecology, the relative importance of eukaryotes (including protists and fungi), FL bacteria and PA bacteria in constructing the microbial network and whether the response of their network to cyanobacterial bloom is consistent with the properties of these networks remain largely unknown.

Freshwater microorganisms exhibit large compositional and functional variability following cyanobacterial blooms (Liu et al., 2019a; Woodhouse et al., 2016; Xue et al., 2017). Cyanobacteria are biological drivers of nutrient cycling in freshwater ecosystems (Cottingham et al., 2015; Gao et al., 2022). Large amounts of dissolved organic matter can be released into the water column owing to mass release from senescent cyanobacterial cells, and this provides a subsidy of both carbon and nitrogen to the microbial food web (Aoki et al., 2008; Cottingham et al., 2015). The resultant shift of plankton food web structure, such as predation and parasitism, during the cyanobacterial blooms, will promote changes in ecosystem processes associated with nutrient cycling (Chow et al., 2014; Gerphagnon et al., 2015; Karpowicz et al., 2020). For example, high cyanobacterial biomass in bloom periods can result in elevated rates of nitrification, denitrification, anaerobic ammonium oxidation, and carbon sequestration (Peng et al., 2017; Sandrini et al., 2014; Xue et al., 2017). Our recent work revealed that high cyanobacterial biomass can regulate allochthonous resource use (carbon) and inter-taxonomic group variation of reservoir zooplankton community (Gao et al., 2022). Some studies have linked microbial interactions to the nutrient cycling in terrestrial and mountain ecosystems based on network features (Chen et al., 2022; Jiao et al., 2021). However, whether and how the cyanobacterial-associated microbial cross-kingdom network complexity and stability affect microbial functional structure have not been studied so far.

To understand how cyanobacterial blooms affect the relationships between the network structures among protists, fungi and different size-fractionated bacteria and community functional structure, we examined the dynamics of associations among eukaryotic plankton, FL bacteria and PA bacteria in a subtropical reservoir during and after a cyanobacterial bloom using an ecological network approach. We aimed to: (1) evaluate the relative importance of eukaryotic plankton, FL bacteria and PA bacteria for the stability of the microbial network; (2) reveal the environmental factors that drive eukaryotes-bacteria associations following the cyanobacterial bloom; (3) profile the difference of microbial networks from bloom to post-bloom periods in terms of network

complexity; (4) uncover potential relationships of the connections between keystone species and network structure with key functional structure on carbon and nitrogen cycling. Due to a stronger response by PA than FL bacteria and activity to cyanobacterial blooms based on the findings of our previous study (Liu et al., 2019b), we hypothesize that eukaryotes would exhibit a stronger linkage to PA bacteria than to FL bacteria and that their dynamics might also be critical for maintaining microbial network complexity and nutrient (carbon and nitrogen) cycling.

2. Materials and methods

2.1. Sample collection

A total of 18 water samples were collected in Xidong Reservoir (24°49' N, 118°10' E) twice a month from October 2014 to December 2014 (Xue et al., 2017). Three different water layers were sampled: surface (0.5-m depth), middle (12-, 14-, 17-, 17-, 20- and 18-m depth for the six sampling days, respectively) and bottom (25-m depth) (Xue et al., 2018). Cyanobacterial blooms dominated by the *Microcystis* occurred in the Xidong Reservoir during the first two sampling days in October, and three well-defined phases reflected the transition from cyanobacterial bloom to post-bloom periods based on the phytoplankton community succession and cyanobacterial biomass, that is, bloom period, post-bloom period 1, and post-bloom 2 period (Fig. S1). Three major microbial size fractions were collected using polycarbonate filters (47 mm diameter, Millipore, Billerica, MA, USA): eukaryotes (>0.22 µm), free-living (FL) bacteria (0.2–3 µm) and particle-attached (PA) bacteria (>3 µm). These filters were stored at – 80 °C until DNA and RNA extractions. The environmental parameters of the waters were measured and analyzed as described previously (Xue et al., 2017).

2.2. DNA and RNA extractions, and real-time quantitative PCR

DNA and RNA extractions from filters were carried out as previously described (Liu et al., 2019b; Xue et al., 2018). The copies of eukaryotic plankton 18S rRNA gene were quantified using the LightCycler 480 Real-Time PCR System (Roche, Rotkreuz, Switzerland). A total of 20 µL PCR reaction mixtures included 10 µL of SYBR Premix ExTaq™ (Takara Bio Inc., Kusatsu, Japan), 7.2 µL of RNase-free water, 0.4 µL of every 10 µM primer (PCR primers: 1380F and 1510R, the same primers as 18S rRNA gene sequencing), and 2 µL of DNA. PCR amplification condition was as follows: incubation at 94 °C for 30 s, and 40 cycles of 5 s for 94 °C, 15 s for 50 °C and 10 s for 72 °C (Mo et al., 2021). All the PCR reactions were performed in triplicate throughout the experiment, and negative controls were set up. Standard curve was constructed using 10-fold gradient dilutions of plasmids including an insert fragment of the *Cryptomonas pyrenoidifera* (cryptophyte) gene. The amplification efficiency of the standard curve was 108.5 % in this study. Both 16S rDNA copies and its transcript (16S rRNA copies) were quantified as previously described (Liu et al., 2019b). The rRNA-rDNA ratios were roughly used for estimating the transcriptional activity of the bacterial community.

2.3. Illumina sequencing, metagenomic sequencing and bioinformatics

Eukaryotic and bacterial high-throughput sequencing and bioinformatics methods were described in detail in our previous papers (Liu et al., 2019b; Xue et al., 2018). Eukaryotic and bacterial sequences were rarefied to 123,090 sequences and 36,152 sequences per sample, respectively. The raw sequence data have been submitted to the Sequence Read Archive (SRA) of NCBI under BioProject numbers PRJNA348137 for eukaryotes and PRJNA315049 for bacteria.

A total of 12 samples from the surface and bottom waters were selected for metagenomic sequencing. Metagenomic libraries were prepared using NEBNext Ultra DNA Library Prep Kit for Illumina (New England Biolabs, Ipswich, MA, USA) following the manufacturer's

instruction. Libraries sequencing was performed on the Illumina HiSeq2500 platform using 2×150 bp paired-end sequencing approach (Illumina Inc., San Diego, CA, USA). A total of 129,514.62 Mbp raw reads (10,792.89 Mbp reads per sample on average) for 12 samples were obtained. To get the clean reads, raw reads were processed by removing adaptor-contaminated (≥ 15 bp sequence overlap with adapter sequence), ambiguous (≥ 10 ambiguous nucleotides) and low-quality reads (≥ 40 nucleotides with quality score below 38). Finally, 129,117.47 Mbp clean reads (about 10 Gb of clean reads data per sample on average) were obtained for further functional analysis (Liu et al., 2019c). Clean reads were merged and assembled using SOAP denovo, and obtained Scaffolds (≥ 500 bp). We used MetaGeneMark to predict and filter open reading frame (ORF), and finally produced a gene catalogue (Unigenes) for further analysis. DIAMOND software was used to map Unigenes with each functional database (KEGG Orthology and eggNOG databases). Here, we mainly focused on carbon and nitrogen cycling-related genes, including carbon degradation, carbon fixation and nitrogen cycling functions (Ploug et al., 2010). For each functional gene, relative abundance was calculated based on the sum sequencing depth of every gene with the total sequence number of all genes per sample. All metagenomic sequence data have been uploaded in the public NCBI database under the BioProject number PRJNA416667.

Protists were roughly assigned as consumers, parasites, phototrophs and unknown taxa (Adl et al., 2019; Simon et al., 2015). Consumers (e.g., ciliates) comprised some protists mainly feeding on bacteria and fungi. Parasites mainly comprised Perkinsea, Ichthyosporea and Peronosporomycetes. Phototrophs comprised some protists which can obtain energy via photosynthesis, such as chlorophytes and cryptophytes. Protists with undetermined functions traits were classified as “unknown” taxa (9.41 % of the total eukaryotic OTUs and 5.80 % of the total eukaryotic sequences).

2.4. Molecular ecological network construction

To avoid biases of correlation calculation, we only chose OTUs with >10 sequences in all samples to include in the network analysis in this study. The filtered OTUs included 1356 eukaryotic OTUs, 1121 FL bacterial OTUs and 1397 PA bacterial OTUs, respectively. Eukaryotic, FL bacterial and PA bacterial co-occurrence network was constructed using Spearman rank correlation based on an RMT-based approach determining the similarity threshold (Yuan et al., 2021; Zhou et al., 2010). These analyses were performed using the Molecular Ecological Network Analysis Pipeline (MENAP, <https://ieg4.rccc.ou.edu/MENAP/>). Network-level (nodes, links, average degree, density and modularity) and node-level (degree and betweenness) topological properties were estimated using MENAP (Deng et al., 2012). To identify the topological roles of network nodes, we calculated within-module connectivity (Z_i) and among-module connectivity (P_i) for each node, and then all nodes were classified as module hubs ($Z_i \geq 2.5, P_i < 0.62$), network hubs ($Z_i \geq 2.5, P_i \geq 0.62$), connectors ($Z_i < 2.5, P_i \geq 0.62$) and peripherals ($Z_i < 2.5, P_i < 0.62$) (Xue et al., 2018; Yuan et al., 2021). Subnetworks for each sample were generated using the *subgraph* function with igraph package (Csárdi and Nepusz, 2006). Further, several network-level topological properties (node number, edge number, average degree, average path length, average betweenness, density, transitivity, modularity and diameter) were estimated per sample with the igraph package.

2.5. Statistical analyses

To assess the relative importance of protists, fungi, metazoa, FL bacteria and PA bacteria in constructing the microbial network, we measured statistical differences in node-level features among the different taxa using Wilcoxon rank sum tests. We used the Mantel test to calculate the Pearson's correlation between module eigenvalue and environmental variables with the vegan R package. The network robustness analysis was conducted using the “attacking” nodes in the

static network based on random nodes (species) removal (Peng and Wu, 2016; Yuan et al., 2021). To test if the subnetwork topological properties changed over time, we measured linear correlations between each topological feature and sampling days (day of year) using the *lm* function with ggpubr R package. We calculated the Spearman correlations between subnetwork-level topological properties and environmental variables, microbial diversity, abundance and 16S rDNA transcriptional activity. Finally, Spearman correlations were analyzed between keystone taxa and functional genes (carbon degradation, carbon fixation and N cycling) as well as network topological properties using the *picante* package in R. Networks were visualised in Gephi 0.9.2.

3. Results

3.1. General overview of the microbial network

The whole microbial network consisted of 1349 nodes and 4774 links (Fig. 1A, B). There were more intra-kingdom links than inter-kingdom linkages, and most of the intra-kingdom links were positive (Fig. 1B). Importantly, there were about three times as many eukaryotic connections with particle-attached (PA) bacteria (187 links) than with free-living (FL) bacteria (66 links), and most of these links were negative. We mainly found some negative correlations between protists (e.g., Ciliophora, Chlorophyta and Cryptophyta) and PA bacteria (Acidobacteria, Bacteroidetes, Chloroflexi, Firmicutes and Proteobacteria). The negative relationship between eukaryotes and FL bacteria was mainly classified into protists (e.g., Ciliophora) and Acidobacteria, Firmicutes and Proteobacteria (Fig. S2). Our network showed a high degree of modularity (0.75), and 72.6 % of the nodes were accounted for by only 11 of the 149 total modules (Fig. S3A). Eukaryotes were distributed into 11 major modules, while FL and PA bacteria were mainly located in modules 2, 3, 4, 5, 7 and 11 (Fig. S3B). A total of 24 nodes within the ecological network were classified as keystone nodes (i.e., connectors and module hubs), including 10 eukaryotes, 3 FL bacteria and 11 PA bacteria (Fig. S3A; Table S1). Connectors were found in modules 1, 2, 4, 5 and 10 and mainly classified as 6 eukaryotes (Cerczoza, Chlorophyta, Ciliophora and Diatomea) and 1 PA bacterium (Betaproteobacteria) (Fig. S3B; Table S1). The module hubs mainly included 3 FL bacteria and 10 PA bacteria belonging to the phyla Actinobacteria, Acidobacteria, Cyanobacteria, Chlorobi and Proteobacteria, and mainly occurring in the modules 2, 3, 4, 5 and 7 (Fig. S3B; Table S1). Additionally, there were four module hubs belonging to Cerczoza (1 OTU), Chlorophyta (2 OTUs) and unidentified Stramenopiles (1 OTU).

3.2. The contribution of eukaryotes to community stability

Overall, the degree value was significantly higher ($P < 0.05$; Wilcoxon rank sum tests) for protists (consumers, phototrophs and unknown groups) than for PA bacteria and FL bacteria (Fig. 1C). The betweenness value was significantly higher ($P < 0.05$; Wilcoxon rank sum tests) for protists (consumers, phototrophs and unknown groups) than for FL bacteria, while there was no significant difference between protists and PA bacteria. We further verified the importance of eukaryotes in constructing the microbial network using the network robustness. Network robustness with absence of eukaryotes was significantly lower than that of networks where FL bacteria or PA bacteria were removed (Fig. S4A).

3.3. Dynamics of the microbial network community following cyanobacterial bloom

Module eigenvalue can act as a proxy for the collective abundance of its members, and for most modules, their patterns were closely correlated with the environmental changes (Fig. S5). Modules 1, 4 and 5 were significantly positively correlated with pH, chlorophyll *a*, total carbon and total organic carbon, but negatively correlated with nitrite nitrogen.

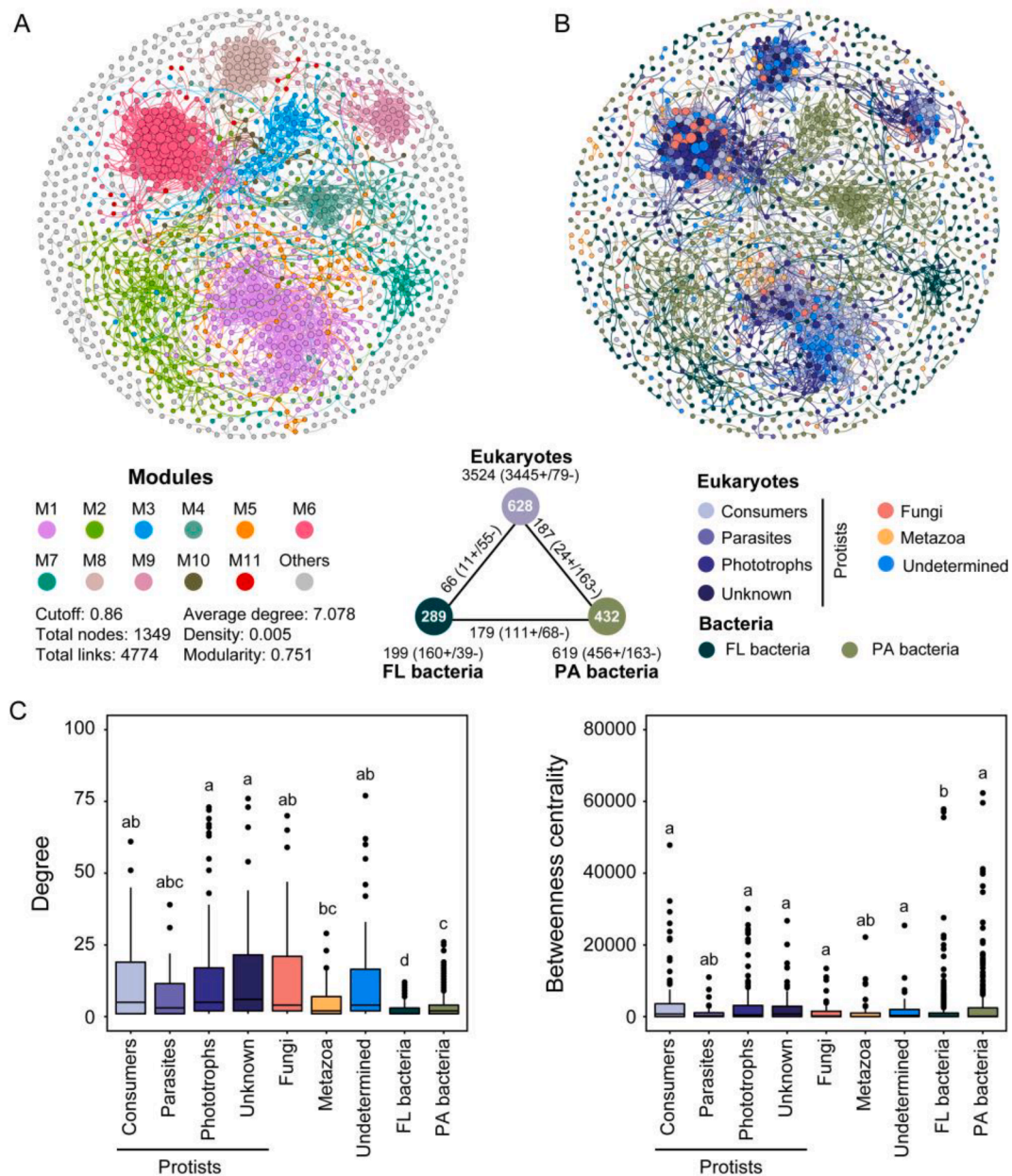


Fig. 1. Co-occurrence patterns of eukaryotic and size-fractionated bacterial taxa following a cyanobacterial bloom in Xidong Reservoir. FL bacteria and PA bacteria represent free-living and particle-attached bacteria, respectively. meta-community co-occurrence network with nodes coloured according to module classes (A) and microbial taxa (B). A connection stands for a strong (Pearson's $r \geq 0.86$ or $r \leq -0.86$) and significant ($P < 0.05$) correlation. The size of each node is proportional to the number of connections (i.e., degree). A summary of node-edge statistics is provided to bottom middle of the network. Numbers inside the coloured circles represent the number of nodes in corresponding categories. Numbers outside the coloured circles indicate the number of inner connections in corresponding categories, and the numbers above the edges represent the number of cross-group interactions. Plus (+) and minus (-) indicate positive and negative connections, respectively. Eukaryotes were classified into protists, fungi and metazoa. Protists are further assigned into four main functional groups: consumers, parasites, phototrophs and unknown taxa. Undetermined taxa mean eukaryotic supergroups could not be discriminated. Comparison of unique node-level topological features for different microbial taxa (C). Different letters indicate significant differences at the $P < 0.05$ level based on Wilcoxon rank sum tests.

Module 3 was strongly negatively correlated with water temperature, pH, chlorophyll *a*, total carbon and total organic carbon. Ternary plot analysis indicated that most major modules were specific (relatively more abundant) for bloom or post-bloom periods (Fig. 2A). The OTUs from modules 1, 3, 4, 5, 6, 8 and 9 were grouped into cyanobacterial bloom or post-bloom periods. The OTUs from other modules (2, 7, 10 and 11) were uniformly distributed in three different periods (bloom, post-bloom 1 and post-bloom 2).

Module diversity mirrored the community shift from cyanobacterial bloom to post-bloom periods (Fig. 2B, Fig. S6). Within module 1, a significant decrease appeared in the relative abundance of consumers

(Cercozoa and Ciliophora), phototrophs (Chlorophyta, Chrysophyceae and Cryptophyceae) and metazoa from the bloom to the post-bloom periods. The relative abundance of Actinobacteria (PA bacteria) also decreased. Module 3 was dominated by PA bacteria, and the abundance of Proteobacteria significantly increased from the bloom to the post-bloom periods, while consumers (Ciliophora) showed the reverse pattern. Module 4 was dominated by PA bacteria, and the abundances of Bacteroidetes, Cyanobacteria and Proteobacteria significantly declined following the bloom. Similarly, module 5 was dominated by PA bacteria, and the abundance of Bacteroidetes significantly declined following the bloom. However, the abundances of phototrophs (Chlorophyta and

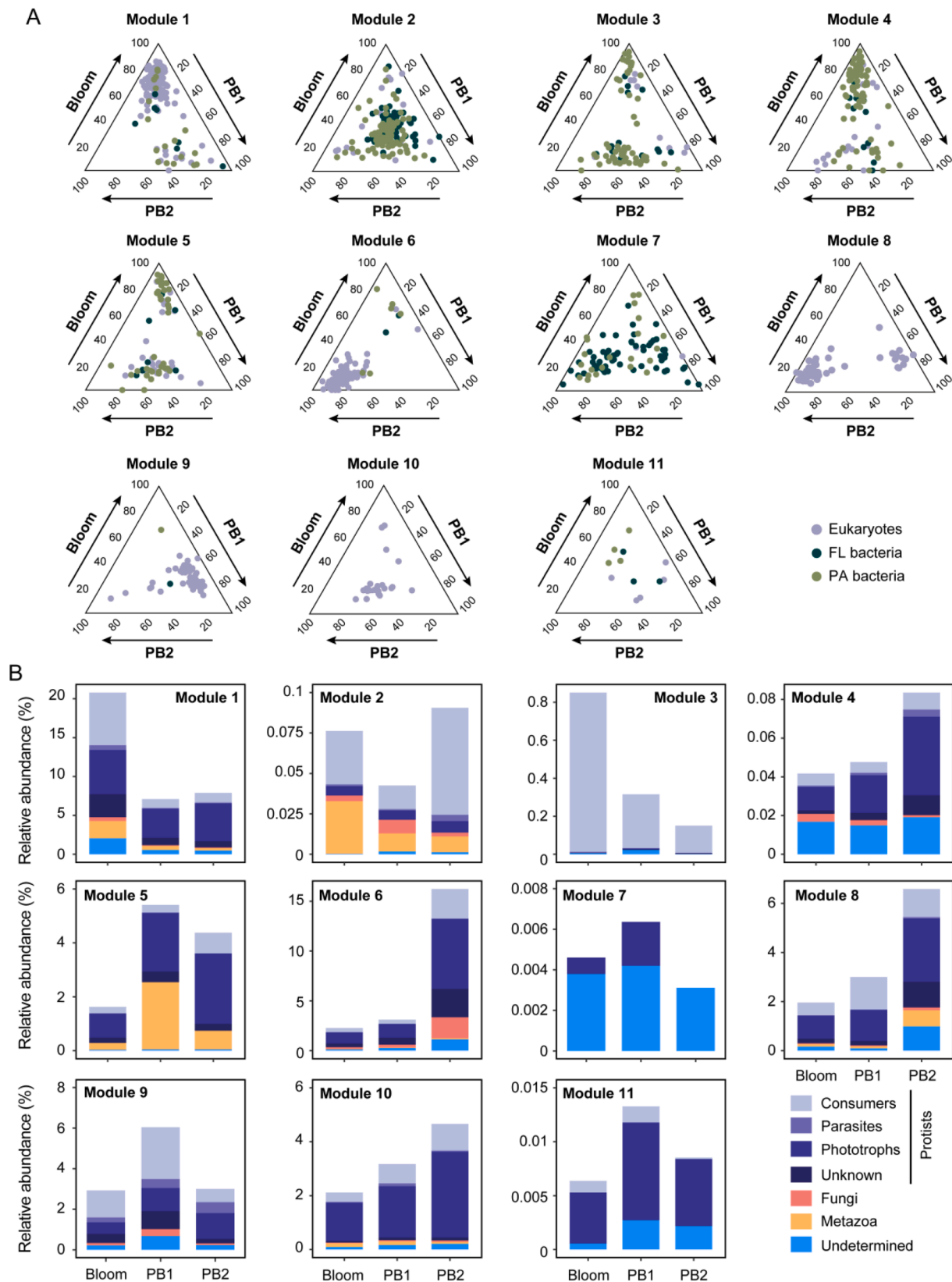


Fig. 2. Relative abundance of eukaryotic and bacterial OTUs from major modules in the three different succession periods. Ternary plots showing relative abundance of eukaryotes, free-living (FL) bacteria and particle-attached (PA) bacteria for major modules from cyanobacterial bloom to post-bloom periods (A). Each node represents one OTU. For each OTU, abundance was averaged over all samples for each period. Accumulated relative abundances of eukaryotic taxa for each major module (B). PB1 and PB2 indicate post-bloom 1 and post-bloom 2 period, respectively.

Cryptophyta) showed the opposite pattern. Module 6 was dominated by eukaryotes, and the abundances of consumers, phototrophs and fungi significantly increased from the bloom to the post-bloom periods. Module 8 only had eukaryotes, and the abundances of phototrophs (Cryptophyta, Cryptophyceae) progressively and significantly increased from the bloom period to period 2. Module 9 was dominated by protists (Chlorophyta, Chrysophyceae and Ciliophora), which exhibited the highest relative abundances in post-bloom period 1.

3.4. Changes in network complexity and stability over time

To determine whether cyanobacterial blooms affected microbial network complexity and stability, the changes of various network topological properties were regressed against time (Fig. 3; Fig. S4B). Network edge number (edge number; $R^2 = 0.708$, $P < 0.05$), average degree (average D; $R^2 = 0.845$, $P < 0.01$), edge density ($R^2 = 0.703$, $P < 0.05$) and robustness ($R^2 = 0.918$, $P < 0.01$) strongly increased over time from the cyanobacterial bloom to the non-bloom periods. However, network modularity ($R^2 = 0.879$, $P < 0.01$) significantly decreased over time from cyanobacterial bloom to non-bloom periods. The other intriguing question is how cyanobacterial blooms decreased network complexity, which we addressed using three analyses. First, the network topology properties (e.g., edge number, degree, density and transitivity) exhibited strong negative correlations with water temperature, pH, total carbon and total organic carbon, while modularity was positively correlated with cyanobacterial bloom-related variables including pH, chlorophyll *a*, total carbon and total organic carbon (Fig. S7A). Second, the changes in network structure (e.g., edge number, degree, density and transitivity) were tightly negatively associated with FL bacterial 16S rRNA copies and with PA bacterial 16S rRNA copies and the rRNA-rDNA ratios (Fig. S7B). However, modularity demonstrated the reverse patterns. Third, some keystone eukaryotes (OTU_572 Ciliophora, OTU_110 Cercozoa, OTU_12 and OTU_332 Diatomea) and PA bacteria (OTU_177 Actinobacteria, OTU_658 Chlorobi, OTU_72 Firmicutes, OTU_170 Deltaproteobacteria) exhibited a significant and positive effect on the network structure (e.g., edge number, degree and density) (Fig. S8). Degree and density were significantly negatively correlated with keystone eukaryote (OTU_702 Chlorophyta) and PA bacteria (OTU_22 Cyanobacteria, OTU_51 and OTU_82 Alphaproteobacteria). We also found that keystone eukaryotes (OTU_702, OTU_24, and OTU_188 Chlorophyta), PA bacteria (OTU_22 Cyanobacteria, OTU_51 and OTU_82 Alphaproteobacteria) and FL bacteria (OTU_39 Deltaproteobacteria) were significantly and positively correlated with modularity (Fig. S7). However, OTU_572 (Ciliophora), OTU_110 (Cercozoa), OTU_12 and OTU_332 (Diatomea), OTU_250 (PA bacteria Deltaproteobacteria) and OTU_133 (PA bacteria Gammaproteobacteria) were significantly and negatively correlated with the modularity.

3.5. Relationships between network structure and key element cycling

Potential microbial functions (i.e., carbon and nitrogen cycling genes) were assessed by metagenomics. Specifically, the relative abundances of eukaryotic and PA bacterial hubs had more significant links with the relative abundances of the nitrogen cycling genes, followed by carbon degradation and fixation genes, than keystone FL bacterial hubs (Fig. 4A; Table S2). Interestingly, there were more significant correlation pairs between network indices, especially network modularity, and the relative abundances of nitrogen cycling genes, followed by carbon fixation and carbon degradation genes (Fig. 4B; Table S3). Considering their correlated links, the proportion of negative correlations was greater than the number of positive correlations.

4. Discussions

Cyanobacterial blooms are an extensively studied environmental disturbance that can severely impact the services and functions of reservoir ecosystems (Barros et al., 2019; Leigh et al., 2010). Previous studies have shown that the genetic diversity and activity of aquatic microorganisms vary in complex patterns in response to environmental changes and interspecies interactions induced by cyanobacterial blooms, further influencing ecological resilience (Amorim et al., 2020; Gao et al., 2022; Liu et al., 2019b; Woodhouse et al., 2018). The genetic composition and metabolism of bacterial communities differ at micro-scale level in aquatic ecosystems, for example particle-attached (PA) niches and free-living (FL) niches (Ganesh et al., 2014; Tang et al., 2017). However, only interactions within bacteria within different size fractions (FL and PA) or eukaryotes in bulk waters during cyanobacterial blooms, have been explored in previous network analyses (Chun et al., 2020; Liu et al., 2019a; Yang et al., 2017). In this study, we mainly focused on the change of cross-trophic correlations among FL bacteria, PA bacteria and protists during and after a cyanobacterial bloom.

4.1. Mechanisms that eukaryotes play major ecological roles in maintaining eukaryotes-bacteria interactions

We used microbiome network analysis to visualize the scenarios of microbial interactions during and after a cyanobacterial bloom. The network topological features can be used for evaluating the roles of microbial interactions (Jiao et al., 2019; Xue et al., 2018). Our results demonstrated that eukaryotes (particularly protists) were more often at the core of the cross-trophic network than PA and FL bacterial taxa due to higher values of topological features (i.e., degree and betweenness). Eukaryotic plankton as key components of aquatic food webs, plays multiple ecological roles in primary production, predation and parasitism (Worden et al., 2015). More importantly, protists are operating as

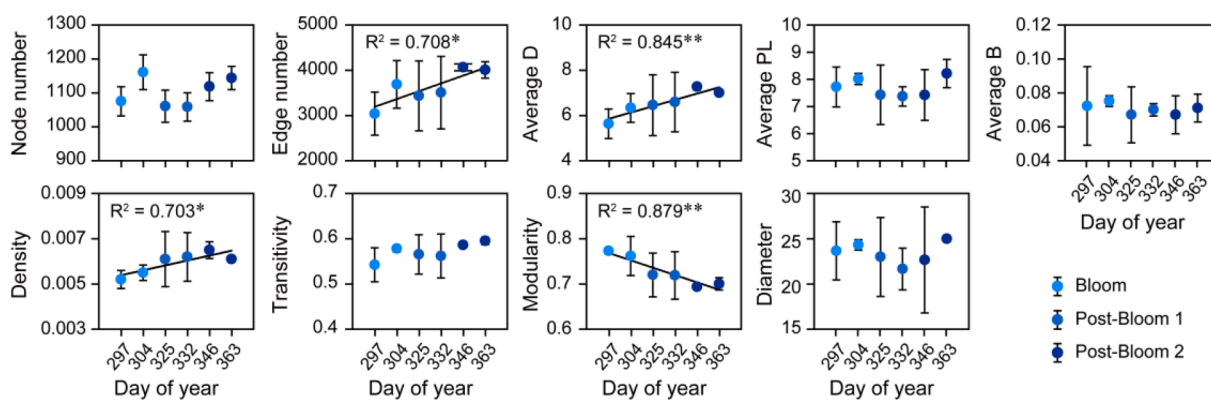


Fig. 3. Temporal changes of network properties from cyanobacterial bloom to post-bloom periods. Sampling period was shown using day of year. Average D, average degree; Average PL, average path length; Average B, average betweenness. Only significant adjusted R^2 values from linear regressions are shown ($*P < 0.05$; $**P < 0.01$).

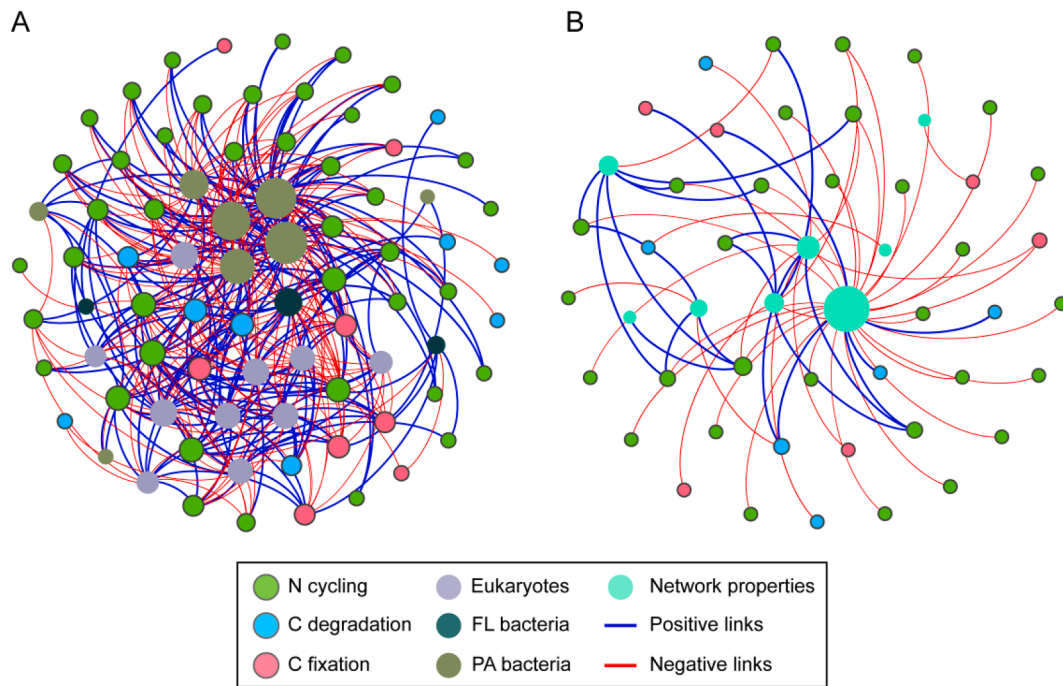


Fig. 4. Spearman correlations of keystone OTU relative abundances (A), network topological properties (B) and relative abundances of carbon fixation, carbon degradation and nitrogen cycling genes. The annotations of the carbon fixation, carbon degradation and nitrogen cycling genes are listed in **Table S2** and **Table S3**. A connection stands for a strong (Spearman's $r \geq 0.5$ or $r \leq -0.5$) and significant ($P < 0.05$) correlation. The thickness of the line indicates the strength of the correlation between two nodes. The size of each node is proportional to the number of connections (i.e., degree per node). The network topological properties are as shown in **Fig. 3**.

pivotal regulators of microbial community structure, activities and evolution through their predation on bacteria and fungi and other microeukaryotes (Pernthaler, 2005; Sherr and Sherr, 2002). Given these important ecological roles of the eukaryotic plankton, they may be more often at network center than other taxa. Furthermore, we found that most connector taxa in the co-occurrence network belonged to the functional groups of protists: consumers (Cercozoa and Ciliophora) and phototrophs (Chlorophyta and Diatomea). Previous studies have shown that these eukaryotic plankton species responded markedly to the dynamics of cyanobacterial blooms and were dominant in network modules (Liu et al., 2019a; Xue et al., 2018). The extinction of connectors may cause fragmentation of the entire network into isolated modules (Olesen et al., 2007), which may well be explained why removing eukaryotes greatly affected the connectivity of the cross-trophic network in this study.

Our network analysis revealed that eukaryotic taxa had more interactions with PA bacteria than with FL bacteria. Potential explanations may be the existence of traits associated with PA bacteria, such as higher metabolic activity and a stronger response to cyanobacterial blooms by PA than FL bacteria (Liu et al., 2019b), and this may underlie more eukaryotic-PA bacterial links. Moreover, particle-associated microbial communities contain a higher proportion of eukaryotic plankton taxa; for example, heterotrophic protists, fungi and metazoa (Duret et al., 2020; Poff et al., 2021). Thus, the bacteria attached to particles may be overall closer to eukaryotes than FL bacteria due to smaller spatial distances. This presumably reflects the fact that eukaryotes live in close association with PA bacteria in nutrient-replete particle microhabitats. Additionally, in our study, the eukaryotic communities had more negative associations with PA bacteria. We speculate that a cyanobacterial bloom can facilitate the PA bacterial production because exudation and cell lysis can result in the increase in easily degradable organic carbon (Bock et al., 2020); on the other hand, the cyanobacterial bloom can boost some rare bacteria (e.g., Actinobacteria, Bacteroidetes, and Firmicutes) shifts from FL to PA lifestyles, therefore, further intensifying protists and microzooplankton preying on bacteria (Liu et al.,

2019b). Our results highlight that the eukaryotic taxa (especially protists) as potential key controllers may contribute to the increase of network stability following the cyanobacterial bloom.

4.2. Mechanisms that the cyanobacterial bloom could influence the inter-domain network

First, network module eigenvalues showed positive or negative significant associations with water temperature, pH, chlorophyll *a*, total carbon, total organic carbon and nitrite nitrogen. Environmental variables can impact species co-occurrence by generating highly correlated clusters (e.g., modules or guilds) in ecological networks (Röttjers and Faust, 2018). Microbial members of modules may tightly correlate or tolerate similar environmental conditions (Chafee et al., 2018). The physicochemical factors in the reservoirs were significantly correlated with the cyanobacterial biomass (Liu et al., 2019b; Xue et al., 2018). Both nutrients and temperature are important factors influencing cyanobacterial bloom intensification and diversification (Jankowiak et al., 2019; Lv et al., 2014). The quick change in cyanobacterial biomass could be related to a significant shift in eukaryotic and bacterial abundance and community composition, further triggering a series of dynamic changes among different microorganisms. Therefore, the changes in network structure might result from the effect of cyanobacterial blooms on the surrounding environment.

Second, cyanobacterial blooms can modify the trophic structure by top-down or bottom-up control, and several modules were found in the cross-kingdom network. In each major module, mostly dominated by eukaryotes or PA bacteria or both, the changes in protistan consumers likely follow the changes in the bacterial communities as bacteria are their main food sources. These major modules corresponded well with the three cyanobacterial succession periods. For instance, the taxa of modules 1 and 3 had highest relative abundance in the cyanobacterial bloom period, dominated by Ciliophora and/or Cercozoa, which are main consumers of bacteria, and algal blooms will strengthen the rate of bacterial production and growth (Engström-Öst et al., 2013). Thus,

increasing abundance of the phylum Ciliophora could be due to the increase in the abundance of their food source. Moreover, our network analysis showed strong negative correlations between bacterivores (e.g., Ciliophora) and the bacterial communities (mainly Proteobacteria and Bacteroidetes), providing indirect evidence for protist preying on bacteria. Research has shown that protists prefer some gram-negative bacteria, such as alpha-proteobacteria, beta-proteobacteria and Bacteroidetes (Asiloglu et al., 2021). Additionally, we observed the increase in abundance of some phototrophic groups (e.g., Chlorophyta and Cryptophyta) in some major modules after the end of the cyanobacterial bloom. Phototrophic protists dominated the phytoplankton community after the collapse of the cyanobacterial bloom, giving support for a shift to a non-cyanobacterial taxa-dominated state after the cyanobacterial bloom. Additionally, functional groups of protists encompassing consumers and phototrophs exhibited a synchronous increase in some major modules that were dominated by positive correlations likely due to synergistic interactions. The shift in cyanobacterial biomass can have mixed effects, either inhibiting (via the predation) or promoting (via the supply of dissolved organic carbon) growth of certain bacteria or eukaryotes causing a sequential change in the food web structure.

Third, both network complexity and stability significantly increased after the cyanobacterial bloom. This result supports a central ecological belief that complexity begets stability (Okuyama and Holland, 2008). Some environmental factors (water temperature, pH, chlorophyll *a* and total carbon) exhibited a significant negative association with network complexity (e.g., edge number, degree and density). Every OTU may exhibit distinct co-occurrence patterns with environmental changes. Therefore, correlations between the reservoir microbial plankton were dynamic along temporal environmental gradient. Importantly, FA bacterial 16S rRNA copies and PA bacterial 16S rDNA transcriptional activity (16S rRNA copies and the rRNA-rDNA ratios) showed significant negative associations with edge number, degree and density, and these network indices significantly increased after the cyanobacterial bloom. Our previous study demonstrated that FL and PA bacterial abundances and PA bacterial 16S rDNA transcriptional activity during the bloom period was significantly higher than those during the post-bloom period (Liu et al., 2019b), which is in line with the resource-copy number theory (“more resource, more copy number”) (Lauro et al., 2009). Microbial activity and resource availability are important drivers of microbial network structures (Shi et al., 2016). Furthermore, trophic correlations might be more dominant in nutrient-poor than in nutrient-rich ecosystems, because high nutrient availability results in the increasing importance of the bottom-up control further driving microbial community composition (Lenoir et al., 2007; Moore et al., 2003). The decrease in resource availability (carbon and nitrogen resources) may contribute to stronger interactions between microbes following the cyanobacterial blooms.

4.3. Keystone eukaryotes and PA bacteria determined network structure and ecological functions

Some generalist eukaryotes and PA bacteria (connectors and module hubs) showed significantly positive or negative relationships with network complexity indices. These keystone members usually had higher connectivity within or between modules (Deng et al., 2012) and contributed to shaping network structure (Banerjee et al., 2018). This provides direct evidence that eukaryotes and PA bacteria determine more of the network structure than FL bacteria. Another important finding was that the keystone groups were related to the carbon and nitrogen cycling genes. Previous findings have suggested that the functional capacities of particular taxa have a greater influence on the ecosystem characteristics than the total number of species because specific functioning (e.g., nitrification and denitrification) is only attributed to a fraction of species (Jiao et al., 2019; Jiao et al., 2022). For example, eukaryotic hubs, including Cercozoa, Chlorophyta, Ciliophora and Diatomea have been reported to participate in the dissolved organic

carbon metabolism and the nitrogen biogeochemical cycle (Jiao et al., 2010; Lundgaard et al., 2017; Zhao et al., 2021). Cyanobacteria (PA bacterial hub) can provide organic carbon used for N₂ production (Fuchsman et al., 2019). Previous studies showed that these PA bacterial hubs, including Acidobacteria, Firmicutes, Alphaproteobacteria, Betaproteobacteria, Gammaproteobacteria, and Deltaproteobacteria contributed with large proportions to nitrogenase genes or denitrification genes in subtropical reservoirs (Wang et al., 2015; Yu et al., 2014). Sharp decrease in the cyanobacterial abundance was associated with changes in the relative abundance of keystone species (e.g., Cercozoa, Ciliophora, Actinobacteria, Bacteroidetes and Proteobacteria). We assume that these keystone eukaryotes and PA bacteria are reservoir ecosystem engineers that shape network structure and function.

Our findings have important implications for predicting ecological consequences of frequent cyanobacterial blooms and so for reservoir ecosystem management. During the bloom period, algal exudates represent an important carbon source (Bock et al., 2020). The increase in easily degradable organic carbon paves the way for fast-growing bacteria and intensifies interactions between indicator bacteria and some eukaryotes. Protistan grazing on bacteria play an essential role in transferring carbon and energy to higher trophic levels (Gerphagnon et al., 2015). Cyanobacterial blooms could accelerate the nitrogen cycle due to the elevated rates of nitrification, denitrification and anaerobic ammonium oxidation (Peng et al., 2017; Xue et al., 2017), which may then decrease eutrophication level in nitrogen-limited ecosystems and promote bloom regression in deep reservoirs (Xue et al., 2017). The amount of carbon and nitrogen in the reservoir gradually decreased accompanied by the disappearance of the cyanobacterial bloom, in tandem with the synchronous changes in the abundance and community of heterotrophic bacteria and protists, further having the potential to alter nutrient cycling. PA bacteria generally include genes enabling multiple metabolic capabilities due to large and variable genomes, and PA bacterial cells can well utilize patches of organic matter and grow rapidly during algal blooms (Luo and Moran, 2015). Recent research indicated that bacteria and eukaryotes enriched on particle play central roles in carbon export and nitrogen transfer (Boeuf et al., 2019; Poff et al., 2021). Here, some eukaryotic and PA bacterial hub species had more strongly positive or negative correlations with carbon or nitrogen cycling genes, suggesting they might largely boost carbon and nitrogen transfer in this ecosystem.

5. Conclusions

We found that microbial network co-occurrence patterns varied substantially from the cyanobacterial bloom to post-bloom periods, and the plankton network complexity and stability significantly increased with cyanobacterial bloom collapse. The changes in the protistan communities induced by cyanobacterial bloom had more negative interactions with PA bacterial communities, suggesting that protists may exhibit top-down control on the PA bacteria communities, with implications for various ecosystem functional processes. Moreover, key eukaryotic and PA bacterial species contributed importantly to the network structure and consequently to the carbon and nitrogen cycling. Thus, the cyanobacterial function as ecological engineers controlling the co-occurrence patterns of the other microbes. Importantly, we highlight that the size of the particles is vital for determining microbial network structure, and the use of different size-fractions provides a more comprehensive insight of the correlations between cross-trophic microbes.

Declaration of Competing Interest

The authors declare that they have no known competing financial interests or personal relationships that could have appeared to influence the work reported in this paper.

Data availability

Data will be made available on request.

Acknowledgements

The work was funded by the National Natural Science Foundation of China (32001152, 92047204 and 32100331), the Natural Science Foundation of Fujian Province of China (2020J01119 and 2020J05089), the Science & Technology Basic Resources Investigation Program of China (2017FY100300) and the Environmental Protection Science & Technology Project of Fujian Province of China (2021R009 and 2022R002). EJ was funded by the TÜBITAK program BIDEB2232 (118C250). We thank David M. Wilkinson and Anne Mette Poulsen for English editing.

Appendix A. Supplementary data

Supplementary data to this article can be found online at <https://doi.org/10.1016/j.ecolind.2022.109401>.

References

- Adl, S.M., Bass, D., Lane, C.E., Lukeš, J., Schoch, C.L., Smirnov, A., et al., 2019. Revisions to the classification, nomenclature, and diversity of eukaryotes. *J Eukaryotic Microbiol* 66, 4–119.
- Amorim, C.A., Dantas, É.W., do Nascimento Moura, A., 2020. Modeling cyanobacterial blooms in tropical reservoirs: the role of physicochemical variables and trophic interactions. *Sci Total Environ* 744, 140659.
- Aoki, S., Ohara, S., Kimura, K., Mlzuguchi, H., Fuse, Y., Yamada, E., 2008. Characterization of dissolved organic matter released from *Microcystis aeruginosa*. *Anal Sci* 24, 389–394.
- Asiloglu, R., Kenya, K., Samuel, S.O., Sevilir, B., Murase, J., Suzuki, K., et al., 2021. Top-down effects of protists are greater than bottom-up effects of fertilisers on the formation of bacterial communities in a paddy field soil. *Soil Biol Biochem* 156, 108186.
- Baltar, F., Palovaara, J., Unrein, F., Catala, P., Hornák, K., Šimek, K., et al., 2016. Marine bacterial community structure resilience to changes in protist predation under phytoplankton bloom conditions. *ISME J* 10, 568–581.
- Banerjee, S., Schlaeppi, K., van der Heijden, M.G.A., 2018. Keystone taxa as drivers of microbiome structure and functioning. *Nat Rev Microbiol* 16, 567–576.
- Barros, M.U.G., Wilson, A.E., Leitão, J.I.R., Pereira, S.P., Buley, R.P., Fernandez-Figueroa, E.G., et al., 2019. Environmental factors associated with toxic cyanobacterial blooms across 20 drinking water reservoirs in a semi-arid region of Brazil. *Harmful Algae* 86, 128–137.
- Bjorbaekmo, M.F.M., Evenstad, A., Rosage, L.L., Krabberød, A.K., Logares, R., 2020. The planktonic protist interactome: where do we stand after a century of research? *ISME J* 14, 544–559.
- Bock, C., Jensen, M., Forster, D., Marks, S., Nuy, J., Psenner, R., et al., 2020. Factors shaping community patterns of protists and bacteria on a European scale. *Environ Microbiol* 22, 2243–2260.
- Boeuf, D., Edwards, B.R., Eppley, J.M., Hu, S.K., Poff, K.F., Romano, A.E., et al., 2019. Biological composition and microbial dynamics of sinking particulate organic matter at abyssal depths in the oligotrophic open ocean. *Proc Natl Acad Sci USA* 116, 11824–11832.
- Chafee, M., Fernández-Guerra, A., Buttigieg, P., Gerds, G., Eren, A.M., Teeling, H., et al., 2018. Recurrent patterns of microdiversity in a temperate coastal marine environment. *ISME J* 12, 237–252.
- Chen, W.Q., Wang, J.Y., Chen, X., Meng, Z.X., Xu, R., Duoji, D.Z., et al., 2022. Soil microbial network complexity predicts ecosystem function along elevation gradients on the Tibetan Plateau. *Soil Biol Biochem* 172, 108766.
- Chow, C.E., Kim, D.Y., Sachdeva, R., Caron, D.A., Fuhrman, J.A., 2014. Top-down controls on bacterial community structure: microbial network analysis of bacteria, T4-like viruses and protists. *ISME J* 8, 816–829.
- Chun, S.J., Cui, Y.S., Lee, J.J., Choi, I.C., Oh, H.M., Ahn, C.Y., 2020. Network analysis reveals succession of *Microcystis* genotypes accompanying distinctive microbial modules with recurrent patterns. *Water Res* 170, 115326.
- Cottingham, K.L., Ewing, H.A., Greer, M.L., Carey, C.C., Weathers, K.C., 2015. Cyanobacteria as biological drivers of lake nitrogen and phosphorus cycling. *Ecosphere* 6, 1–19.
- Csárdi, G., Nepusz, T., 2006. The igraph software package for complex network research. *Inter J Comp Syst* 1695, 1–9.
- Deng, Y., Jiang, Y.H., Yang, Y.F., He, Z.L., Luo, F., Zhou, J.Z., 2012. Molecular ecological network analyses. *BMC Bioinformatics* 13, 113.
- Duret, M.T., Lampitt, R.S., Lam, P., 2020. Eukaryotic influence on the oceanic biological carbon pump in the Scotia Sea as revealed by 18S rRNA gene sequencing of suspended and sinking particles. *Limnol Oceanogr* 65, S49–S70.
- Eloe, E.A., Shulse, C.N., Fadrosch, D.W., Williamson, S.J., Allen, E.E., Bartlett, D.H., 2011. Compositional differences in particle-associated and free-living microbial assemblages from an extreme deep-ocean environment. *Environ Microbiol Rep* 3, 449–458.
- Engström-Ost, J., Autio, R., Setälä, O., Sopanen, S., Suikkanen, S., 2013. Plankton community dynamics during decay of a cyanobacteria bloom: a mesocosm experiment. *Hydrobiologia* 701, 25–35.
- Fuchsmann, C.A., Palevsky, H.I., Widner, B., Duffy, M., Carlson, M.C.G., Neibauer, J.A., et al., 2019. Cyanobacteria and cyanophage contributions to carbon and nitrogen cycling in an oligotrophic oxygen-deficient zone. *ISME J* 13, 2714–2726.
- Ganesh, S., Parris, D.J., DeLong, E.F., Stewart, F.J., 2014. Metagenomic analysis of size-fractionated picoplankton in a marine oxygen minimum zone. *ISME J* 8, 187–211.
- Gao, X.F., Wang, W.P., Ndayishimiye, J.C., Govaert, L., Chen, H.H., Jeppesen, E., et al., 2022. Invasive and toxic cyanobacteria regulate allochthonous resource use and community niche width of reservoir zooplankton. *Freshwater Biol* 67, 1344–1356.
- Gerphagnon, M., Macarthur, D.J., Latour, D., Gachon, C.M.M., Van Ogtrop, F., Gleason, F.H., et al., 2015. Microbial players involved in the decline of filamentous and colonial cyanobacterial blooms with a focus on fungal parasitism. *Environ Microbiol* 17, 2573–2587.
- Grujic, V., Nuy, J.K., Salcher, M.M., Shabarova, T., Kasalicky, V., Boenigk, J., et al., 2018. Cryptophyta as major bacterivores in freshwater summer plankton. *ISME J* 12, 1668–1681.
- Guimerà, R., Amaral, L.A.N., 2005. Functional cartography of complex metabolic networks. *Nature* 433, 895–900.
- Huisman, J., Codd, G.A., Paerl, H.W., Ibelings, B.W., Verspagen, J.M.H., Visser, P.M., 2018. Cyanobacterial blooms. *Nat Rev Microbiol* 16, 471–483.
- Jankowiak, J., Hattenrath-Lehmann, T., Kramer, B.J., Ladds, M., Gobler, C.J., 2019. Deciphering the effects of nitrogen, phosphorus, and temperature on cyanobacterial bloom intensification, diversity, and toxicity in western Lake Erie. *Limnol Oceanogr* 64, 1347–1370.
- Jiao, S., Chen, W.M., Wei, G.H., 2022. Core microbiota drive functional stability of soil microbiome in reforestation ecosystems. *Global Change Biol* 28, 1038–1047.
- Jiao, N.Z., Herndl, G.J., Hansell, D.A., Benner, R., Kattner, G., Wilhelm, S.W., et al., 2010. Microbial production of recalcitrant dissolved organic matter: long-term carbon storage in the global ocean. *Nat Rev Microbiol* 8, 593–599.
- Jiao, S., Xu, Y.Q., Zhang, J., Hao, X., Lu, Y.H., 2019. Core microbiota in agricultural soils and their potential associations with nutrient cycling. *mSystems* 4, e00313-18.
- Jiao, S., Peng, Z.H., Qi, J.J., Gao, J.M., Wei, G.H., 2021. Linking bacterial-fungal relationships to microbial diversity and soil nutrient cycling. *mSystems* 6, e01052-20.
- Karpowicz, M., Zieliński, P., Grabowska, M., Ejsmont-Karabin, J., Kozłowska, J., Feniova, I., 2020. Effect of eutrophication and humification on nutrient cycles and transfer efficiency of matter in freshwater food webs. *Hydrobiologia* 847, 2521–2540.
- Lauro, F.M., McDougald, D., Thomas, T., Williams, T.J., Egan, S., Rice, S., et al., 2009. The genomic basis of trophic strategy in marine bacteria. *Proc Natl Acad Sci USA* 106, 15527–15533.
- Leigh, C., Burford, M.A., Roberts, D.T., Udy, J.W., 2010. Predicting the vulnerability of reservoirs to poor water quality and cyanobacterial blooms. *Water Res* 44, 4487–4496.
- Lenoir, L., Persson, T., Bengtsson, J., Wallander, H., Wirén, A., 2007. Bottom-up or top-down control in forest soil microcosms? Effects of soil fauna on fungal biomass and C/N mineralisation. *Biol Fertil Soils* 43, 281–294.
- Liu, L.M., Chen, H.H., Liu, M., Yang, J.R., Xiao, P., Wilkinson, D.M., et al., 2019a. Response of the eukaryotic plankton community to the cyanobacterial biomass cycle over 6 years in two subtropical reservoirs. *ISME J* 13, 2196–2208.
- Liu, M., Liu, L.M., Chen, H.H., Yu, Z., Yang, J.R., Xue, Y.Y., et al., 2019b. Community dynamics of free-living and particle-attached bacteria following a reservoir *Microcystis* bloom. *Sci Total Environ* 660, 501–511.
- Liu, X., Xiao, P., Guo, Y.Y., Liu, L.M., Yang, J., 2019c. The impacts of different high-throughput profiling approaches on the understanding of bacterial antibiotic resistance genes in a freshwater reservoir. *Sci Total Environ* 693, 133585.
- Liu, S.W., Yu, H., Yu, Y.H., Huang, J., Zhou, Z.Y., Zeng, J.X., et al., 2022. Ecological stability of microbial communities in Lake Donghu regulated by keystone taxa. *Ecol Indic* 136, 108695.
- Lundgaard, A.S.B., Treusch, A.H., Stief, P., Thamdrup, B., Glud, R.N., 2017. Nitrogen cycling and bacterial community structure of sinking and aging diatom aggregates. *Aquat Microb Ecol* 79, 85–99.
- Luo, H.W., Moran, M.A., 2015. How do divergent ecological strategies emerge among marine bacterioplankton lineages? *Trends Microbiol* 23, 577–584.
- Lv, H., Yang, J., Liu, L.M., Yu, X.Q., Yu, Z., Chiang, P.C., 2014. Temperature and nutrients are significant drivers of seasonal shift in phytoplankton community from a drinking water reservoir, subtropical China. *Environ Sci Pollut Res* 21, 5917–5928.
- Mestre, M., Borrull, E., Sala, M.M., Gasol, J.M., 2017. Patterns of bacterial diversity in the marine planktonic particulate matter continuum. *ISME J* 11, 999–1010.
- Mikhailov, I.S., Zakharova, Y.R., Bukin, Y.S., Galachyants, Y.P., Petrova, D.P., Sakirko, M.V., et al., 2019. Co-occurrence networks among bacteria and microbial eukaryotes of Lake Baikal during a spring phytoplankton bloom. *Microb Ecol* 77, 96–109.
- Mo, Y.Y., Peng, F., Gao, X.F., Xiao, P., Logares, R., Jeppesen, E., et al., 2021. Low shifts in salinity determined assembly processes and network stability of microeukaryotic plankton communities in a subtropical urban reservoir. *Microbiome* 9, 128.
- Moore, J.C., McCann, K., Setälä, H., Ruitter, P.C.D., 2003. Top-down is bottom-up: does predation in the rhizosphere regulate aboveground dynamics? *Ecology* 84, 846–857.
- Okuyama, T., Holland, J.N., 2008. Network structural properties mediate the stability of mutualistic communities. *Ecol Lett* 11, 208–216.
- Olesen, J.M., Bascompte, J., Dupont, Y.L., Jordano, P., 2007. The modularity of pollination networks. *Proc Natl Acad Sci USA* 104, 19891–19896.

- Paerl, H.W., Barnard, M.A., 2020. Mitigating the global expansion of harmful cyanobacterial blooms: moving targets in a human- and climatically-altered world. *Harmful Algae* 96, 101845.
- Peng, Y.K., Liu, L., Jiang, L.J., Xiao, L., 2017. The roles of cyanobacterial bloom in nitrogen removal. *Sci Total Environ* 609, 297–303.
- Peng, G.S., Wu, J., 2016. Optimal network topology for structural robustness based on natural connectivity. *Physica A* 443, 212–220.
- Pernthaler, J., 2005. Predation on prokaryotes in the water column and its ecological implications. *Nat Rev Microbiol* 3, 537–546.
- Ploug, H., Musat, N., Adam, B., Moraru, C.L., Lavik, G., Vagner, T., et al., 2010. Carbon and nitrogen fluxes associated with the cyanobacterium *Aphanizomenon* sp. in the Baltic Sea. *ISME J* 4, 1215–1223.
- Poff, K.E., Leu, A.O., Eppley, J.M., Karl, D.M., DeLong, E.F., 2021. Microbial dynamics of elevated carbon flux in the open ocean's abyss. *Proc Natl Acad Sci USA* 118, e2018269118.
- Röttgers, L., Faust, K., 2018. From hairballs to hypotheses—biological insights from microbial networks. *FEMS Microbiol Rev* 42, 761–780.
- Sandrini, G., Matthijs, H.C.P., Verspagen, J.M.H., Muyzer, G., Huisman, J., 2014. Genetic diversity of inorganic carbon uptake systems causes variation in CO₂ response of the cyanobacterium *Microcystis*. *ISME J* 8, 589–600.
- Sherr, E.B., Sherr, B.F., 2002. Significance of predation by protists in aquatic microbial food webs. *Antonie Van Leeuwenhoek* 81, 293–308.
- Shi, S.J., Nuccio, E.E., Shi, Z.J., He, Z.L., Zhou, J.Z., Firestone, M.K., 2016. The interconnected rhizosphere: high network complexity dominates rhizosphere assemblages. *Ecol Lett* 19, 926–936.
- Simon, M., López-García, P., Deschamps, P., Moreira, D., Restoux, G., Bertolino, P., Jardillier, L., 2015. Marked seasonality and high spatial variability of protist communities in shallow freshwater systems. *ISME J* 9, 1941–1953.
- Tang, X.M., Chao, J.Y., Gong, Y., Gong, Y., Wang, Y.P., Wilhelm, S.W., et al., 2017. Spatiotemporal dynamics of bacterial community composition in large shallow eutrophic Lake Taihu: high overlap between free-living and particle-attached assemblages. *Limnol Oceanogr* 62, 1366–1382.
- Wang, L.N., Yu, Z., Yang, J., Zhou, J., 2015. Diazotrophic bacterial community variability in a subtropical deep reservoir is correlated with seasonal changes in nitrogen. *Environ Sci Pollut Res* 22, 19695–19705.
- Woodhouse, J.N., Kinsela, A.S., Collins, R.N., Bowling, L.C., Honeyman, G.L., Hollida, J. K., et al., 2016. Microbial communities reflect temporal changes in cyanobacterial composition in a shallow ephemeral freshwater lake. *ISME J* 10, 1337–1351.
- Woodhouse, J.N., Ziegler, J., Grossart, H.P., Neilan, B.A., 2018. Cyanobacterial community composition and bacteria–bacteria interactions promote the stable occurrence of particle-associated bacteria. *Front Microbiol* 9, 777.
- Worden, A.Z., Follows, M.J., Giovannoni, S.J., Wilken, S., Zimmerman, A.E., Keeling, P. J., 2015. Rethinking the marine carbon cycle: factoring in the multifarious lifestyles of microbes. *Science* 347, 1257594.
- Xu, H.C., Lv, H., Liu, X., Wang, P.F., Jiang, H.L., 2016. Electrolyte cations binding with extracellular polymeric substances enhanced *Microcystis* aggregation: implication for *Microcystis* bloom formation in eutrophic freshwater lakes. *Environ Sci Technol* 50, 9034–9043.
- Xue, Y.Y., Yu, Z., Chen, H.H., Yang, J.R., Liu, M., Liu, L.M., et al., 2017. Cyanobacterial bloom significantly boosts hypolimnetic anammox bacterial abundance in a subtropical stratified reservoir. *FEMS Microbiol Ecol* 93, fix118.
- Xue, Y.Y., Chen, H.H., Yang, J.R., Liu, M., Huang, B.Q., Yang, J., 2018. Distinct patterns and processes of abundant and rare eukaryotic plankton communities following a reservoir cyanobacterial bloom. *ISME J* 12, 2263–2277.
- Yang, C.Y., Wang, Q., Simon, P.N., Liu, J.Y., Liu, L.C., Dai, X.Z., et al., 2017. Distinct network interactions in particle-associated and free-living bacterial communities during a *Microcystis aeruginosa* bloom in a plateau lake. *Front Microbiol* 8, 1202.
- Yu, Z., Yang, J., Liu, L.M., 2014. Denitrifier community in the oxygen minimum zone of a subtropical deep reservoir. *PLoS ONE* 9, e92055.
- Yuan, M.T.M., Guo, X., Wu, L.W., Zhang, Y., Xiao, N.J., Ning, D.L., et al., 2021. Climate warming enhances microbial network complexity and stability. *Nat Clim Change* 11, 343–348.
- Zhao, H.J., Jiang, Y.J., Xiao, Q., Zhang, C., Behzad, H.M., 2021. Coupled carbon-nitrogen cycling controls the transformation of dissolved inorganic carbon into dissolved organic carbon in karst aquatic systems. *J Hydrol* 592, 125764.
- Zhou, J.Z., Deng, Y., Luo, F., He, Z.L., Tu, Q.C., Zhi, X.Y., 2010. Functional molecular ecological networks. *mBio* 1, e00169-10.
- Zhou, Y.Q., Sun, B.Y., Xie, B.H., Feng, K., Zhang, Z.J., Zhang, Z., et al., 2021. Warming reshaped the microbial hierarchical interactions. *Global Change Biol* 27, 6331–6347.